PLANT SCIENCE TODAY
ISSN 2348-1900 (online)
Vol 11(3): 853-863
https://doi.org/10.14719/pst.4521

HORIZON
e-Publishing Group
HePG

RESEARCH ARTICLE

Rice yield prediction through drone-derived vegetation indices: A case study in Tamil Nadu, India

R. Tamilmounika[1], D. Muthumanickam[1*], S. Pazhanivelan[2], K. P. Ragunath[2], R. Kumaraperumal[1] & A. P. Sivamurugan[2]

[1]Department of Remote Sensing & GIS, Tamil Nadu Agricultural University, Coimbatore, Tamil Nadu - 641003, India

[2]Centre for Water & Geospatial Studies, Tamil Nadu Agricultural University, Coimbatore, Tamil Nadu - 641003, India

*Email: muthutnausac@gmail.com

OPEN ACCESS

ARTICLE HISTORY

Received: 02 August 2024
Accepted: 24 August 2024

Available online
Version 1.0 : 16 September 2024
Version 2.0 : 20 September 2024

Check for updates

Additional information

Peer review: Publisher thanks Sectional Editor and the other anonymous reviewers for their contribution to the peer review of this work.

Reprints & permissions information is available at https://horizonepublishing.com/journals/index.php/PST/open_access_policy

Publisher's Note: Horizon e-Publishing Group remains neutral with regard to jurisdictional claims in published maps and institutional affiliations.

Indexing: Plant Science Today, published by Horizon e-Publishing Group, is covered by Scopus, Web of Science, BIOSIS Previews, Clarivate Analytics, NAAS, UGC Care, etc See https://horizonepublishing.com/journals/index.php/PST/indexing_abstracting

CITE THIS ARTICLE

Tamilmounika R,Muthumanickam D, Pazhanivelan S, Ragunath KP, Kumaraperumal R, Sivamurugan AP. Rice yield prediction through drone-derived vegetation indices: A case study in Tamil Nadu, India. Plant Science Today. 2024; 11 (3): 853-863. https://doi.org/10.14719/pst.4521

Abstract

Precision farming has been revolutionized by advancements in drone technology and remote sensing, enabling high accuracy in real-time crop monitoring and yield prediction. To explore the potential of drone-based remote sensing for predicting the rice yield by the assessment of vegetation indice (VI) were generated and analyzed to identify the most sensitive indices for predicting Laef Area Index (LAI), chlorophyll content and biomass. The experiment was conducted in two seasons, *Kuruvai* (July - November 2023) and *Navarai* (December 2023 - March 2024). In *Kuruvai* 2023, a positive correlation was observed between vegetation indices, Wide Dynamic Range Vegetation Index (WDRVI), Modified Chlorophyll and Reflectance Index (MCARI) and Modified Soil Adjusted Vegetation Index (MSAVI) with ground truth biophysical parameters, while *Navarai* season Perpendicular Vegetation Index (PVI), Modified Chlorophyll and Reflectance Index (MCARI) and Green Normalized Difference Vegetation Index (GNDVI) exhibited the highest positive correlation. The multiple linear regression analysis revealed that a combined model incorporating LAI, SPAD chlorophyll and biomass registered the highest R^2 values of 0.792 and 0.800 for the *Kuruvai* and *Navarai* seasons. The predicted yield was positively correlated with the real-time yield with R^2 values of 0.819 and 0.803 for both seasons. This study underscores the potential of drone-based VIs for precise yield prediction, offering a scalable and non-destructive method to enhance agricultural productivity and support decision-making in precision farming. Future research should focus on refining these models for broader applications across crops and agro-climatic conditions.

Keywords

Chlorophyll; drone; indices; remote sensing; yield prediction

Introduction

The agricultural sector has witnessed a transformative shift towards precision farming, driven by technological advancements and data analytics. Real-time crop monitoring and condition assessment help to develop precise management practices to increase yields. The crop yield prediction is helpful for farmers, policymakers and other stakeholders to make informed decisions about planting, harvesting and marketing crops. The conventional yield prediction method relies on historical data, limited spatial resolution and less real-time data and it is time-consuming and labour-intensive (1). In this context, remote sensing data provides real-time monitoring, high spatial resolution, cost-effectiveness and more extensive area coverage (2). With advancements in remote sensing technology,

particularly drones with multispectral sensors, there has been a paradigm shift towards using drone-derived indices for more efficient and precise yield prediction. Drone-based remote sensing offers a non-destructive and scalable approach to monitor crops throughout the growing season and estimate potential yields (3). Yield prediction using drone-derived indices involves collecting, processing and analyzing high-resolution aerial imagery to extract valuable information about crop health, biomass and physiological characteristics. Vegetation indices (VI) strongly correlate the spectral characteristics of crops and their physiological and morphological properties for yield estimation (4).

VI are reflectance values derived from different multispectral bands of wavelengths, *i.e.* blue (440-510nm), green (520-590nm), red (630-685nm), red edge (690-730nm), near-infrared (760-850nm) for intuitive visualization of crop growth status (5). Vegetation indices gives detailed information about the characteristics of vegetation, such as its health, biomass and chlorophyll content. Vegetation Indices are the ratio of the difference between the reflectance of different spectral bands (6) and are very useful in monitoring crop growth and health conditions (3,7). Many VIs have been developed for estimating biophysical variables (8). Canopy reflectance data have created VI to estimate biophysical parameters, *viz.,* LAI, chlorophyll and biomass (9) and by using vegetation indices such as NDVI (Normalized Difference Vegetation Index) (10), GNDVI (Green Normalized Difference Vegetation Index) (11), SAVI (Soil-Adjusted Vegetation Index) (12), NDRE (Normalized Difference Red Edge Index), Transformed Soil Adjusted Vegetation Index (TSAVI) (13), Modified Soil Adjusted Vegetation Index (MSAVI) (14), Difference Vegetation Index (DVI), Green Normalized Difference Vegetation Index (GNDVI), Chlorophyll Index Green (CIG), Chlorophyll Vegetation Index (CVI), Enhanced Vegetation Index (EVI), Leaf Chlorophyll Index (CI), Land Surface Water Index (LSWI) and Triangular greenness index (TGI) predicted the plant physiological parameters for crop yield estimation. Leaf Area Index (LAI) directly influences the photosynthetic activity of crops, which is a crucial driver of biomass production and yield (15). Chlorophyll is the best predictor of plant vigour and health, while the LAI and SPAD Chlorophyll content are directly related to the photosynthetic efficiency of plants. A higher LAI provides more leaf area for photosynthesis, while optimal chlorophyll content ensures efficient light capture and utilization, leading to increased biomass production. These LAI, SPAD Chlorophyll content and biomass are interlinked parameters influencing each other in a complex manner. However, the manual method of measuring these parameters is destructive and time-consuming and obtaining information on spatial context is inaccurate (16-18). Moreover, the prediction of rice yield through drone-based vegetation indices is still lacking. Hence, a two-season study was attempted to test the efficacy of drone technology in capturing high-resolution spectral data for assessing rice yield through vital physiological parameters such as LAI, SPAD chlorophyll and biomass at the spatial level using drone-derived multispectral VIs and validated with ground-based measurements.

Materials and Methods

Study location

The experiment was conducted in the *Kuruvai* (July - November 2023) and *Navarai* (December 2023 - March 2024) seasons at Agricultural Research Station, Bhavanisagar, Erode district of Tamil Nadu, using short-duration rice variety CO 55. It is a short-duration variety (110 - 115 days) with an average yield capacity of 6057 kg/ha. The experimental site is situated at 11.29' N latitude and 77.08' E longitude, at an altitude of 256 m above mean sea level and belongs to the Western agro-climatic zone of Tamil Nadu (Fig. 1).

Image acquisition

Multispectral images were acquired during the maximum tillering stage using DJI Phantom 4 Multispectral drone, as specified in Table 1. It has a gimbal-based imaging system and captures images in the spectral bands viz., Blue: 450 nm, Green: 560 nm, Red: 650 nm, Red Edge: 730 nm, Near-Infrared: 840 nm comprising 1600 x1300 pixel resolution. The flight mission was carried out on September 2023 and February 2024, between 11 AM and 12 noon for multispectral image acquisition.

Ground data collection

The ground data on biomass, LAI and SPAD chlorophyll for 15 points were collected during both seasons at the maximum tillering stage of the crop to validate with the vegetation indices. The sensor, stored in memory, captures the image and then transmits it to the ground station.

The leaf length and breadth of the third leaf from the top and the number of leaves/plants were measured to calculate LAI (19).

$$LAI = \frac{L \times B \times N \times k}{\text{Spacing (cm)}^2} \qquad \text{Eqn. 01}$$

where, L = Mean length of the leaf (cm); B = Mean breadth of the leaf (cm); N = Mean number of leaves plant^{-1}; k = Constant factor (0.75).

Table 1. Specifications of the DJI PM4

Platform	Quadcopter
Max speed	6 m/s
Focal length	5.74 mm
Image size	1600×1300 pixels
Size of the sensor	4.87 x 3.96 mm
Built-in Battery	6000 mAh LiPo 2S
Max Charging Power	160 W
Spectral bands	Spectral bands blue, green, red, red edge, near-infrared

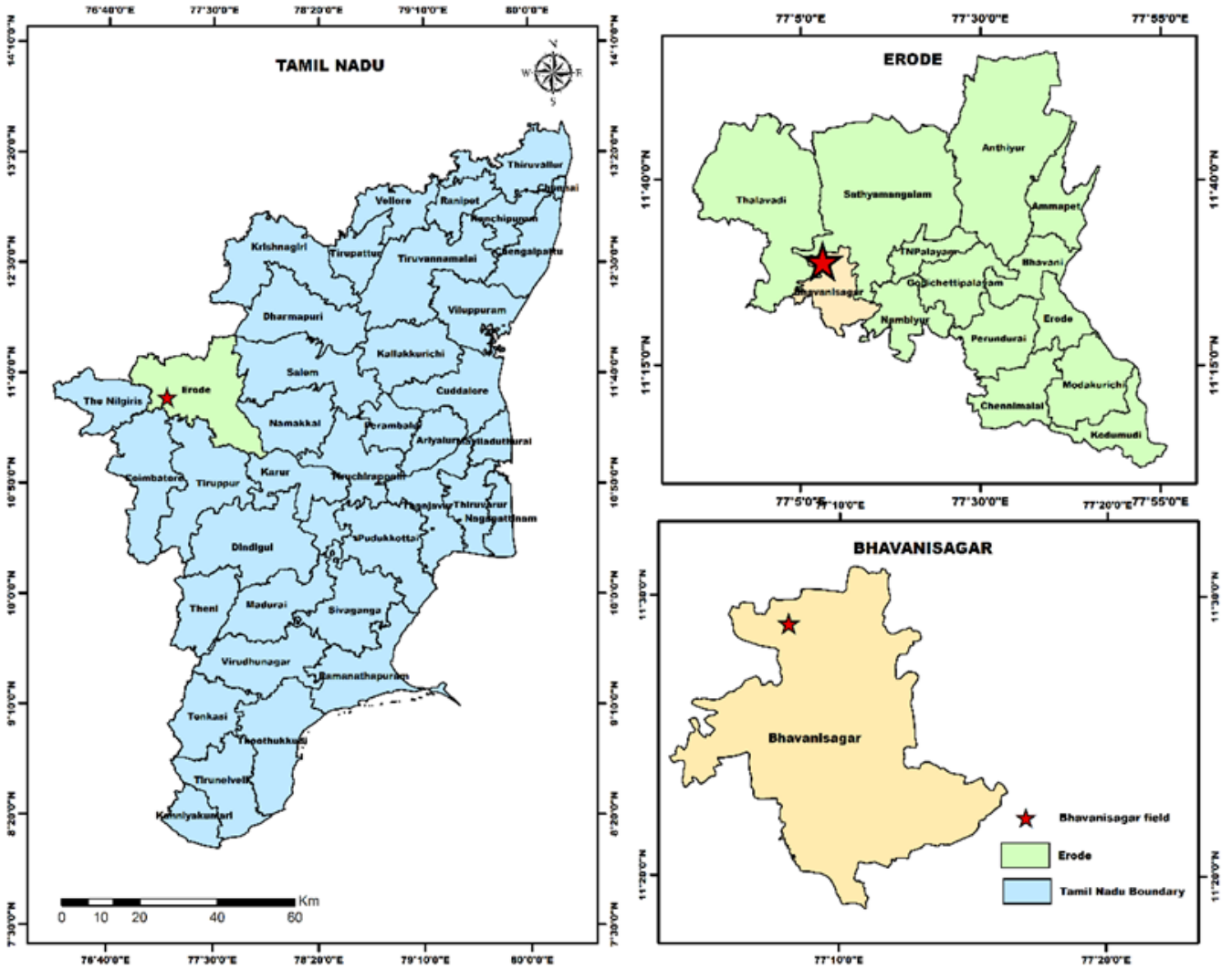

Fig. 1. Location of the study area

The handheld atLEAF CHL PLUS chlorophyll meter (SPAD) was used to measure the light transmittance ratio at 640 nm and 940 nm by adopting a non-destructive method. Biomass was calculated by uprooting, drying and weighing the plant (g/plant). The rice grain yield was recorded during the harvest and expressed in g/plant.

Processing of drone image

Multispectral images captured were processed in Pix4D mapper software. The images were processed, analyzed, and geo-referenced to produce an ortho-mosaic. The multiple overlapped images were stitched together to create an accurate geo-referenced map (Fig. 2). Initial processing, including the images, was added in PIX4D software and automatic tie points were generated in this step. Densified point clouds were created along with automatic tie points and 3D textured mesh was used to generate the Digital Surface Model (DSM) and orthomosaics. The processed false colour composite image is given in Fig 3.

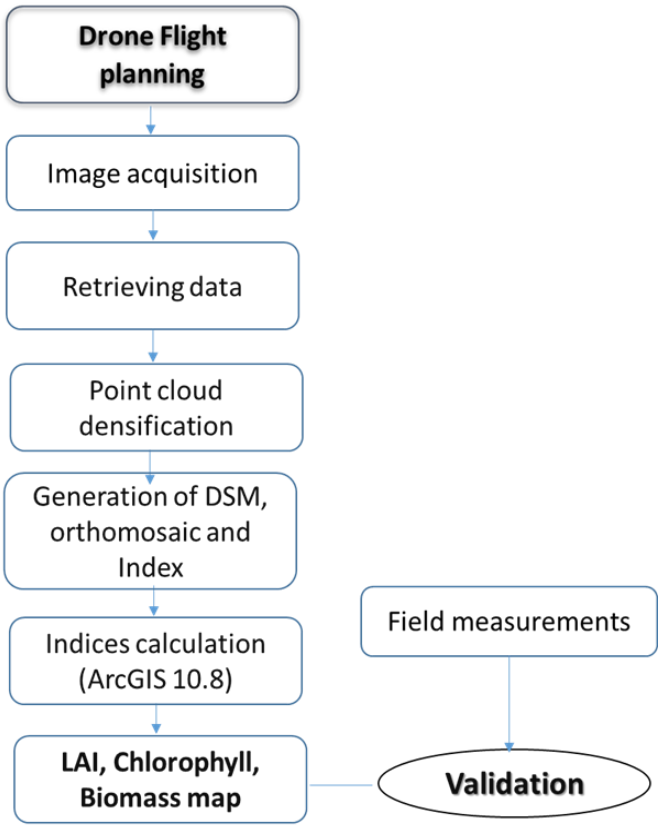

Fig. 2. Flow chart depicting the methodology

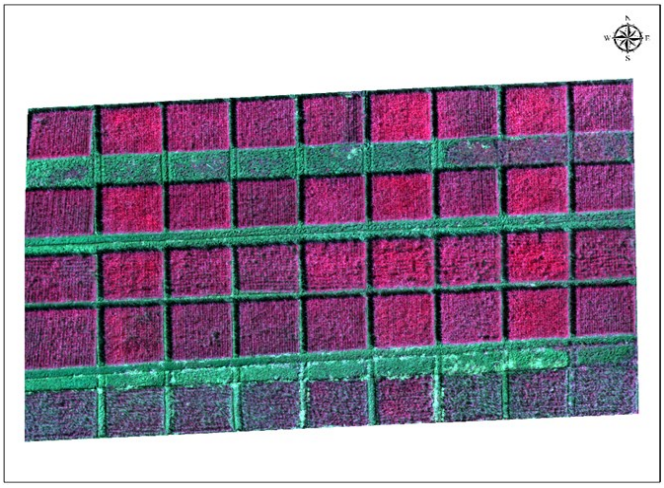

Fig. 3. False Colour Composite image of the field

Vegetation indices generated from drone image

The vegetation indices were generated from the formula using the Raster calculator tool in ArcGIS 10.8 software. Indices like WDRVI, BGI, PVI and ARVI were used in the prediction of LAI, while CI, CVI, TGI and MCARI to predict NDRE, PSRI, MSAVI and GNDVI calculated SPAD chlorophyll values and biomass. The spectral information from different vegetation indices were extracted using the ground truth coordinates (Table 2).

Statistical analysis

Pearson correlation analysis (R) was performed to identify the best vegetation index by correlating it with ground truth data and the coefficient of determination (R^2) to predict the model's accuracy. The regression (R^2) values were calculated for vegetation indices (independent

Table 2. Vegetation indices formula

Index	Equation	Application
Leaf Area Index (LAI)		
Blue-green pigment index (BGI)	B / G	Chlorophyll content and LAI estimation (16)
Perpendicular vegetation index (PVI)	$\sqrt{(0.355\ NIR - 0.149\ R)^2 + (0.355\ R - 0.852\ NIR)^2}$	LAI estimation (20)
Atmospherically resistant vegetation index (ARVI)	$\frac{NIR - (2R - B)}{NIR + (2R - B)}$	LAI estimation, disease infestation and weed mapping (21, 22)
Wide dynamic range vegetation index (WDRVI)	$\frac{0.1\ NIR - R}{0.1\ NIR + R}$	N-Application, LAI, disease infestation (23,24)
SPAD chlorophyll		
Triangular greenness index (TGI)	$G - (0.39 \times R) - (0.61 \times B)$	Chlorophyll content, yield, water content and nitrogen estimation (25,26)
Chlorophyll index (CI)	$\frac{NIR}{RE} - 1$	Chlorophyll and N content (27)
Chlorophyll vegetation index (CVI)	$\frac{NIR}{G} \times \frac{R}{G}$	Crop growth, chlorophyll content, crop yield (28)
Modified chlorophyll and reflectance index (MCARI)	$\frac{RE}{R} \times \{(RE-R) - 0.2\ (RE - G)\}$	Chlorophyll content, Plant health and vigour (28)
Biomass		
Normalized difference red edge index (NDRE)	$\frac{NIR - RE}{NIR + RE}$	Crop health/vigour, Biomass estimation and N management in crops (29)
Modified soil adjusted vegetation index (MSAVI)	$\{2 \times NIR + 1 - \sqrt{(2 \times NIR + 1)^2 - 8 \times (NIR - RED)}\} / 2$	Biomass, N-uptake, Chlorophyll content, Crop yield (30,31)
Plant senescence reflectance index (PSRI)	$\frac{R-G}{RE}$	Biomass, disease infestation, yield and Plant stress (32,33)
Green normalized difference vegetation index (GNDVI)	$\frac{NIR - G}{NIR + G}$	Biomass, Nitrogen content, Water stress, Disease, Yield (30)

(**Note:** B – Blue; G – Green; R – Red; RE – Red Edge; NIR – Near Infrared)

variable) and ground truth data (dependent variable) to assess the best line of fit. RMSE (Root mean square error) determines the average difference between simulations and observations.

$$R = \frac{n\Sigma xy-(\Sigma x)(\Sigma y)}{\sqrt{n\Sigma(x^2)-(\Sigma x^2)}\sqrt{n\Sigma(y^2)-(\Sigma y)^2}} \quad \text{Eqn. 02}$$

$$R^2 = \frac{\sum_{i=1}^{n}(y_i - x_i)^2}{\sum_{i=1}^{n}(y_i - \bar{y})^2} \quad \text{Eqn. 03}$$

$$RMSE = \sqrt{\frac{\sum_{i=1}^{n}(x_i - y_i)^2}{n}} \quad \text{Eqn. 04}$$

The stepwise multiple linear regression was calculated between the independent variables (LAI, SPAD chlorophyll and biomass) and dependent variable (rice yield) in different combinations for two seasons to find the best-fit regression equation for predicting the yield.

Results and Discussion

High-resolution multispectral images acquired during the maximum tillering stage of rice for calculating LAI, biomass and chlorophyll registered strong positive and negative correlations with results. Different vegetation indices viz., WDRVI, BGI, PVI, ARVI, CI, CVI, TGI, MCARI, NDRE, PSRI, MSAVI and GNDVI are used to generate various vegetation indices for two seasons (Tables 3 and 4).

The red wavelength assesses the chlorophyll level and the leaf area index (34). ARVI and WDRVI indices are susceptible to soil noise and lack of sensitivity at high LAI compared with NDVI (35). The WDRVI is a modified version of the NDVI and uses a weighting coefficient to reduce the disparity between near-infrared and red bands (34). Among the four indices used to derive LAI for the *Kuruvai* season, WDRVI was highly correlated with LAI (R = 0.896). WDRVI values ranged from 0.5243 to 0.8996 with a mean of 0.6576 and higher values represent better vegetation health and density. It is more sensitive to leaf area index (LAI) than other indices and enables a more robust characterization of crop physiological and phenological characteristics (36).

The WDRVI was highly correlated with LAI in different vegetation types, including crops, grasslands, and forests. It was less sensitive to atmospheric effects and soil background than other vegetation indices, such as NDVI, making it a more reliable LAI estimation index (37, 38). ARVI registered a mean value of 0.6196, indicating that higher values correspond to healthier and greener vegetation and ARVI is an effective index for atmospheric correction (39). BGI recorded with a mean of 0.3318 indicates the concentration of blue-green pigments in the vegetation, which is associated with healthier and denser vegetation (40). For SPAD chlorophyll, the indices MCARI have a better correlation (R = 0.896) and predicted mean value of 0.0064 and it evaluates the depth of chlorophyll absorption. MCARI is sensitive to variations in chlorophyll concentrations and ground reflectance and the lowest values denote the sensitivity to non-photosynthetic materials and background soil properties in pixel parts (28, 41). MSAVI was a modification of the Soil-Adjusted Vegetation Index (SAVI), which reduces the influence of soil brightness on the vegetation signal (42). MSAVI predicted biomass well compared to other indices (R = 0.909). Values ranged between 0.5062 and 0.5181, with a mean of 0.5116, indicating the presence of healthy vegetation and higher biomass.

Table 3. Vegetation indices value for Kuruvai 2023

S. No.	Lat	Lon	ARVI	BGI	PVI	WDRVI	CI	CVI	MCARI	TGI	MSAVI	PSRI	NDRE	GNDVI
1	11.4833	77.1347	0.6284	0.3221	0.0019	0.4236	0.0486	1.7895	0.0026	0.0002	0.5083	-0.1301	0.0103	0.4512
2	11.4833	77.1350	0.4997	0.3051	0.0020	0.5243	0.0831	1.7801	0.0031	0.0003	0.5062	-0.1057	0.0129	0.4582
3	11.4833	77.1347	0.6475	0.3202	0.0027	0.6221	0.1269	2.2486	0.0030	0.0002	0.5094	-0.0747	0.0151	0.4778
4	11.4834	77.1350	0.5773	0.3018	0.0025	0.5351	0.1829	2.1105	0.0041	0.0004	0.5111	-0.0414	0.0627	0.5300
5	11.4834	77.1348	0.5728	0.3267	0.0026	0.5742	0.2041	3.2229	0.0081	0.0003	0.5068	-0.1372	0.0693	0.5018
6	11.4834	77.1351	0.6036	0.3471	0.0022	0.6913	0.2101	4.3896	0.0094	0.0004	0.5129	-0.0827	0.0796	0.5150
7	11.4832	77.1347	0.4931	0.3124	0.0028	0.6169	0.2204	2.6958	0.0046	0.0004	0.5181	-0.0464	0.0844	0.6210
8	11.4832	77.1350	0.6490	0.3139	0.0030	0.7300	0.2045	2.7590	0.0069	0.0005	0.5120	-0.0905	0.0885	0.5645
9	11.4832	77.1351	0.6065	0.3442	0.0035	0.6501	0.2193	4.1321	0.0080	0.0005	0.5071	-0.0972	0.0917	0.5310
10	11.4834	77.1350	0.7194	0.3394	0.0036	0.7069	0.2970	2.1335	0.0093	0.0006	0.5129	-0.0919	0.1014	0.5888
11	11.4834	77.1348	0.6280	0.3418	0.0028	0.6812	0.3407	2.2426	0.0041	0.0005	0.5152	-0.1062	0.1362	0.6174
12	11.4834	77.1351	0.5426	0.3469	0.0033	0.6042	0.3595	3.3298	0.0069	0.0006	0.5141	-0.0592	0.1588	0.6395
13	11.4833	77.1347	0.7483	0.3482	0.0049	0.8996	0.3324	3.3474	0.0081	0.0005	0.5122	-0.1020	0.1646	0.6132
14	11.4833	77.1350	0.7592	0.3496	0.0048	0.8854	0.4081	3.3734	0.0099	0.0005	0.5147	-0.0318	0.1948	0.7061
15	11.4832	77.1347	0.6179	0.3579	0.0050	0.7199	0.3805	4.1591	0.0082	0.0006	0.5131	-0.0820	0.1607	0.7462
	Mean		**0.6196**	**0.3318**	**0.0032**	**0.6576**	**0.2412**	**2.9143**	**0.0064**	**0.0004**	**0.5116**	**-0.0853**	**0.0954**	**0.5708**

Table 4. Vegetation indices value for *Navarai* 2023-24

S. No.	Lat	Lon	ARVI	BGI	PVI	WDRVI	CI	CVI	MCARI	TGI	PSRI	MSAVI	NDRE	GNDVI
1	11.4833	77.1347	0.6856	0.2459	0.0039	0.7821	0.4749	1.3477	0.0111	0.0004	-0.0970	0.5121	0.1919	0.7128
2	11.4833	77.1349	0.6283	0.2539	0.0039	0.6845	0.4006	1.7075	0.0094	0.0003	-0.1662	0.4098	0.1839	0.6942
3	11.4833	77.1346	0.6254	0.3228	0.0041	0.7402	0.2141	2.5710	0.0146	0.0006	-0.1113	0.5128	0.0967	0.5116
4	11.4834	77.1350	0.8453	0.2618	0.0062	0.8759	0.5022	3.6820	0.0163	0.0005	-0.0156	0.6197	0.2599	0.7636
5	11.4834	77.1347	0.7921	0.4566	0.0069	0.8393	0.3161	4.0216	0.0207	0.0009	-0.0180	0.6217	0.3365	0.8282
6	11.4834	77.1350	0.5788	0.3316	0.0053	0.7026	0.3854	2.7286	0.0157	0.0010	-0.1176	0.4165	0.0848	0.5700
7	11.4832	77.1347	0.6979	0.3638	0.0053	0.7873	0.3426	3.0429	0.0122	0.0004	-0.1024	0.5133	0.1629	0.7419
8	11.4832	77.1349	0.8123	0.3038	0.0055	0.7377	0.6837	5.3384	0.0230	0.0007	-0.0491	0.5949	0.3306	0.7195
9	11.4832	77.1350	0.8073	0.5164	0.0068	0.8334	0.7133	4.7223	0.0210	0.0008	-0.0159	0.6051	0.3936	0.8142
10	11.4834	77.1350	0.5040	0.2611	0.0042	0.5154	0.6403	3.9065	0.0196	0.0006	-0.1035	0.4167	0.1925	0.5494
11	11.4834	77.1347	0.5085	0.1743	0.0032	0.5675	0.4095	2.4768	0.0209	0.0007	-0.1390	0.4167	0.1665	0.7000
12	11.4834	77.1350	0.6604	0.2712	0.0039	0.6983	0.2067	2.4148	0.0116	0.0006	-0.1129	0.4122	0.0937	0.5733
13	11.4833	77.1347	0.6451	0.2775	0.0053	0.7404	0.3310	3.1843	0.0153	0.0007	-0.0695	0.5966	0.2420	0.7441
14	11.4833	77.1349	0.6834	0.2911	0.0059	0.7776	0.6217	3.5280	0.0212	0.0008	-0.1167	0.5184	0.1386	0.6283
15	11.4833	77.1346	0.6442	0.2524	0.0058	0.7506	0.2607	3.1587	0.0094	0.0004	-0.0581	0.7086	0.3153	0.8497
	Mean		**0.6746**	**0.3056**	**0.0051**	**0.7355**	**0.4306**	**3.3202**	**0.0761**	**0.0006**	**-0.0862**	**0.5250**	**0.2126**	**0.6934**

In the *Navarai* season, PVI was correlated well with LAI (R = 0.903). PVI predicted LAI with a mean of 0.0051.PVI was also less sensitive to atmospheric effects and more sensitive to soil brightness, making it effective in removing soil brightness effects for bare soil. It was one of the best predictors of LAI and the performance of the LAI prediction model was improved by using neural network techniques and different data fusion strategies (43). Chlorophyll content was predicted well by MCARI with a minimum and maximum of 0.0094 and 0.0230, respectively, with a mean of 0.0761. MCARI was a chlorophyll-sensitive vegetation index calculated from red and red-edge wavelengths that performed better than other indices. Between 660 and 680nm, a peak in the red region's absorption where the chlorophyll has strong red absorption and near-infrared reflectance peaks (44) and hence MCARI (red and red-edge wavelength) significantly correlate for crop chlorophyll content than other indices (43). These indices are direct proxies for crop biochemistry because the red edge wavelength penetrates deeper into leaf cells than red and blue wavelengths (45). The chlorophyll-specific VIs are more suitable for predicting chlorophyll content (46). GNDVI predicted biomass accumulation compared to other indices and ranged from 0.5116 to 0.8497 with a mean of 0.6934. The GNDVI-based biomass model showed a high level of precision in estimating biomass, with a low RMSE for both fresh and dry biomass (46, 47).

Statistical analysis was carried out to establish a relationship between drone-derived indices and *in-situ* data. The correlation coefficient was calculated to identify the most sensitive index for LAI, biomass and SPAD chlorophyll. The correlation coefficient significantly predicted the vegetation indices WDRVI and PVI for LAI, MSAVI and GNDVI for biomass and SPAD chlorophyll by MCARI. The regression equation (best fit of line) and R^2 values for the vegetation indices were calculated (Table 5).

In the *Kuruvai* season, vegetation indices WDRVI, MCARI and MSAVI had positive correlation coefficient values of 0.896, 0.896 and 0.909, respectively, with the ground truth data. WDRVI, MCARI and MSAVI recorded the R^2 values of 0.803, 0.804 and 0.827, respectively. For the *Navarai* season, PVI, MCARI and GNDVI positively correlated with the ground truth data (R = 0.903, 0.910, 0.908). PVI, MCARI and GNDVI recorded the R^2 values of 0.815, 0.829 and 0.826, respectively and these indices had a higher accuracy for predicting the LAI chlorophyll content and biomass. A higher correlation indicates healthy/dense

Table 5. Relationship between vegetation indices with LAI, SPAD chlorophyll data and biomass

Indices	Regression equation	R^2	Indices	Regression equation	R^2
	Kuruvai			***Navarai***	
			LAI		
ARVI	Y = 3.749x + 0.9486	0.680	ARVI	Y = 3.6733x + 0.3355	0.669
BGI	Y = 13.71x - 1.2779	0.473	BGI	Y = 4.1549x + 1.5436	0.583
PVI	Y = 300.65x + 2.3176	0.705	**PVI**	**Y = 373.3x + 0.9192**	**0.815**
WDRVI	**Y = 2.5607x + 1.5873**	**0.803**	WDRVI	Y = 3.8671x - 0.031	0.626
			SPAD		
CI	Y = 23.594x + 36.829	0.493	CI	Y = 11.286x + 39.199	0.470
CVI	Y = 3.4201x + 32.553	0.666	CVI	Y = 1.9048x + 38.018	0.542
MCARI	**Y = 1272.2x + 34.341**	**0.804**	**MCARI**	**Y = 536.04x + 35.439**	**0.829**
TGI	Y = 19522x + 34.146	0.547	TGI	Y = 10601x + 37.398	0.634
			Biomass		
MSAVI	**Y = 2046.9x - 980.21**	**0.827**	MSAVI	Y = 67.303x + 37.666	0.719
PSRI	Y = 188.98x + 83.116	0.561	PSRI	Y = 119.78x + 83.324	0.527
NDRE	Y = 95.655x + 57.874	0.516	NDRE	Y = 61.607x + 59.901	0.607
GNDVI	Y = 74.385x + 24.542	0.709	**GNDVI**	**Y = 65.933x + 27.283**	**0.826**

vegetation with higher LAI, chlorophyll and biomass. In contrast, lower values indicate stressed/sparse vegetation with lower LAI and chlorophyll content (34, 41). Due to LAI, chlorophyll content and biomass are closely related to the vegetation's ability to absorb and reflect light. As vegetation becomes denser and healthier, it absorbs more light in the visible spectrum and reflects more light in the near-infrared spectrum, leading to higher VI values.

The highly correlated vegetation index WDRVI, PVI, MCARI, MSAVI and GNDVI generate LAI, SPAD chlorophyll and biomass map for both seasons (Fig. 4, 5 and 6). VIs have the potential to predict N deficiency using SPAD values (48) as these indices utilize the same wavebands (640 and 940 nm) used in SPAD meters. WDRVI and MCARI indices are considered the best for calculating LAI and SPAD chlorophyll, respectively and are used to predict the crop's canopy coverage, chlorophyll content and biomass. More leaf area in the image reflects higher SPAD chlorophyll content and biomass (18, 41).

The combination of LAI, SPAD and biomass

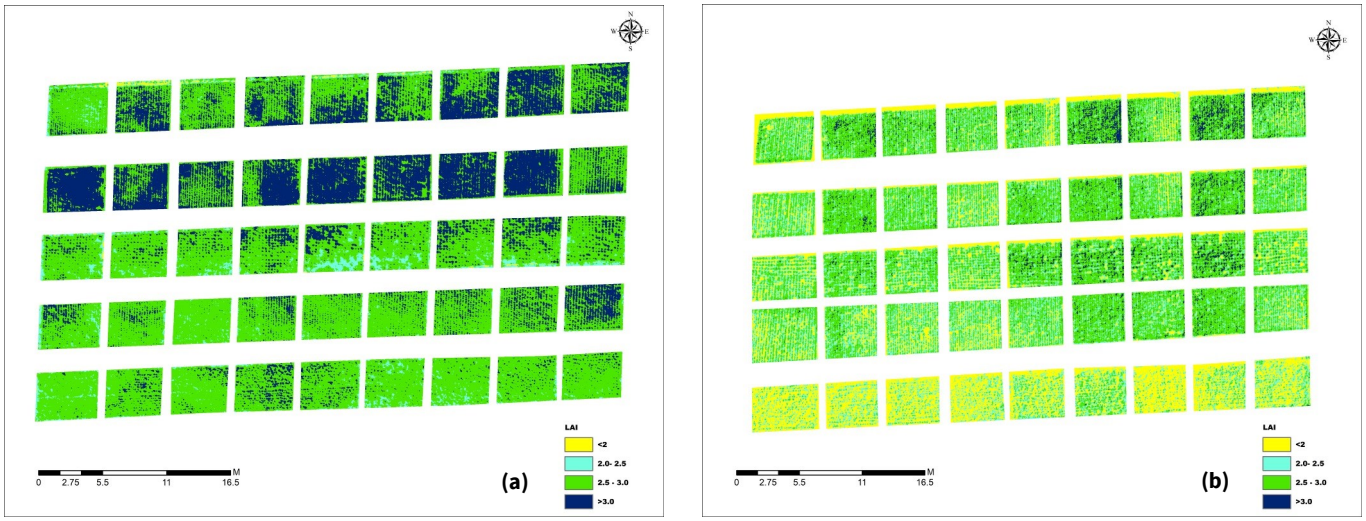

Fig. 4. LAI map for (a) *Kuruvai* season and **(b)** *Navarai* season

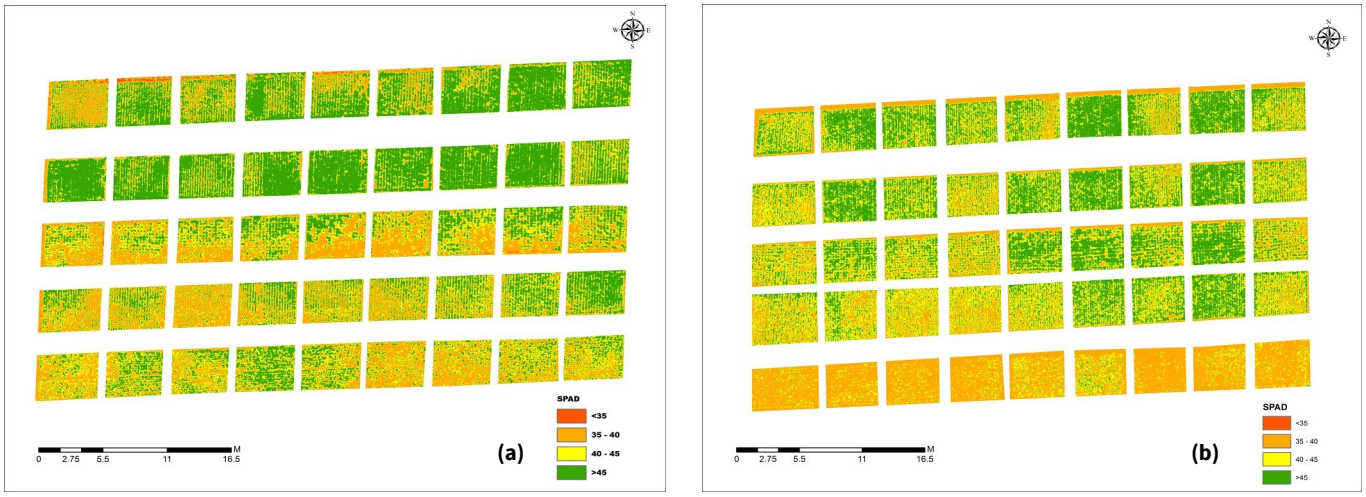

Fig. 5. SPAD chlorophyll map for (a) *Kuruvai* season **and (b)** *Navarai* season

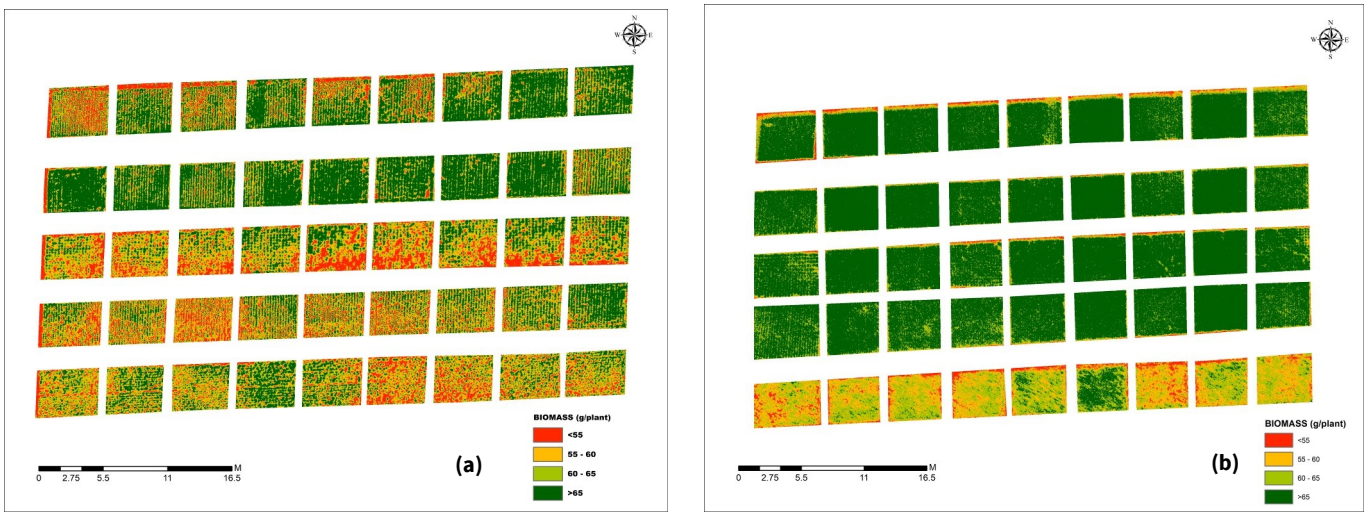

Fig. 6. Biomass (g/plant) map for (a) *Kuruvai* season **(b)** *Navarai* season

regression model registered the highest R^2 value of 0.792 and 0.800 with RMSE 2.342 and 2.368 g/plant for both seasons (Table 6) and reveals that the area with higher LAI, SPAD chlorophyll and biomass predicted more yield, indicating the crop's healthy condition. In comparison, the area with lower LAI and SPAD chlorophyll outlines the stressed condition of the crop with lower yield (34). The yield equation model with a higher R^2 value was further used to generate the rice yield map (Fig. 7). The predicted LAI, SPAD chlorophyll and biomass maps were validated with their ground values for accuracy. The expected yield for the *Kuruvai* and *Navarai* seasons ranged from 25 to 39 and 29 to 42 g/plant, while the observed yield was 32 to 48 and 30 to 45 g/plant, respectively (Table 7). The predicted yield map for combined LAI, SPAD and biomass regression was generated and validated, given in Fig 8.

The crop yield was predicted by plant growth factors, physiological parameters and photosynthesis, which influences chlorophyll, nitrogen concentration and LAI, ultimately affecting vegetation indices, dry matter accumulation and grain yield. The predicted yield positively correlated with the observed yield with R^2 values of 0.819 and 0.803 for both seasons, confirming that yield was influenced by LAI, SPAD chlorophyll and biomass.

Conclusion

This study demonstrated the efficacy of drone-based vegetation indices in predicting rice yield with precision and accuracy. The findings revealed strong correlations between specific vegetation indices and ground truth data for LAI, SPAD chlorophyll and biomass across two rice-growing seasons, *Kuruvai* 2023 and *Navarai* 2023-24. Specifically, WDRVI, MCARI and MSAVI were identified as

Table 6. Relationship of LAI, SPAD chlorophyll and biomass with yield

Attributes	Regression equation	R^2	RMSE	Regression equation	R^2	RMSE
	Kuruvai			*Navarai*		
LAI	Y = 12.308 LAI - 1.467	0.602	2.981	Y = 6.8135 LAI + 17.306	0.689	2.721
SPAD	Y = 0.5317 SPAD + 14.813	0.645	2.815	Y = 0.7622 SPAD + 0.664	0.619	3.010
Biomass	Y = 0.651 Biomass - 2.1302	0.685	2.650	Y = 0.6009 Biomass - 3.6944	0.629	2.969
LAI + SPAD	Y = -1.059 + 7.289 LAI + 0.349 SPAD	0.780	2.304	Y = 18.332 + 7.157 LAI -0.042 SPAD	0.689	2.831
SPAD + Biomass	Y = 2.019 + 0.176 SPAD + 0.457 Biomass	0.696	2.711	Y = -11.236 + 0.476 SPAD + 0.384 Biomass	0.789	2.328
LAI + Biomass	Y = -10.241 + 6.468 LAI + 0.440 Biomass	0.779	2.307	Y = 2.061 + 4.461 LAI+0.331 Biomass	0.798	2.281
LAI + SPAD + Biomass	Y = -5.880 + 6.520 LAI - 0.188 SPAD + 0.232 Biomass	0.792	2.342	Y = -2.247 + 3.094 LAI + 0.160 SPAD+0.340 Biomass	0.800	2.368

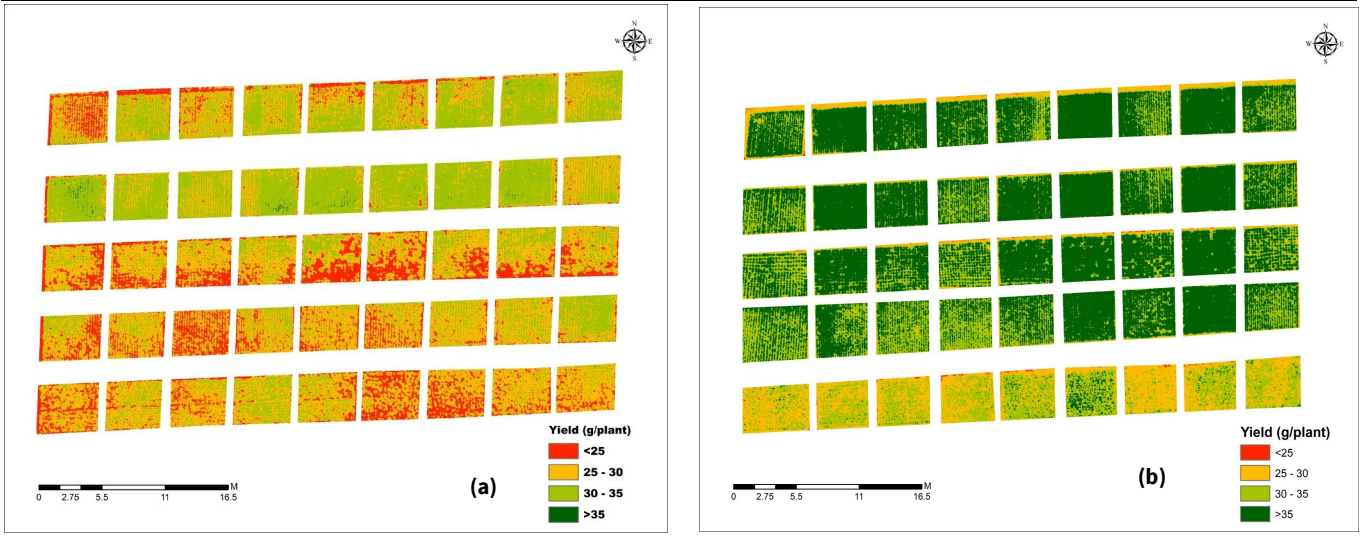

Fig. 7 Predicted yield (g/plant) map using LAI, SPAD and Biomass for (a) *Kuruvai* season **(b)** *Navarai* season

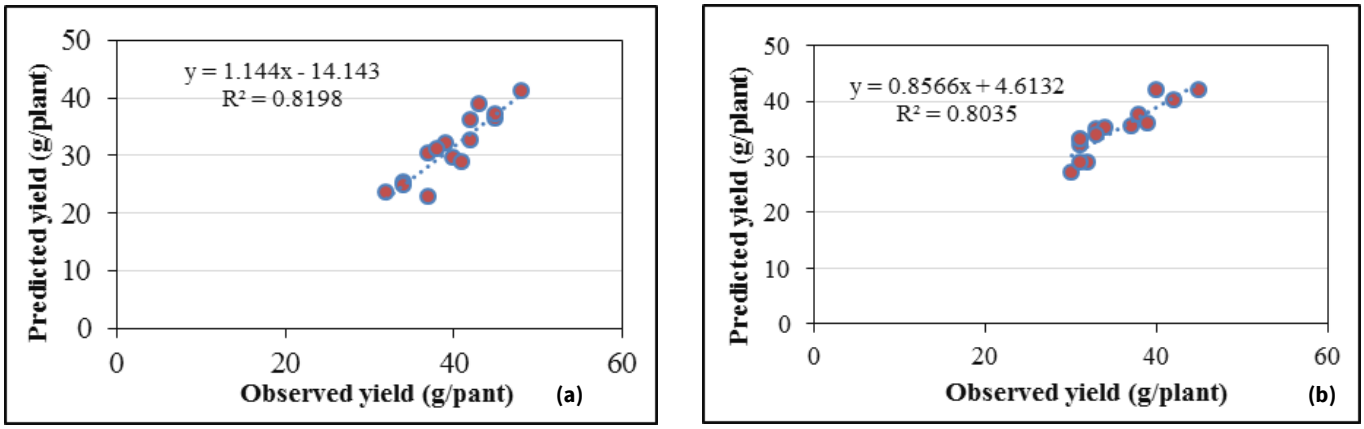

Fig. 8. Accuracy assessment between observed and predicted yield from a combination of LAI, SPAD and biomass **(a)** *Kuruvai* season **(b)** *Navarai* season

Table 7. Observed and predicted yield calculated from the combination of LAI, SPAD chlorophyll and biomass

S. No	*Kuruvai* season (yield g/plant)		*Navarai* season (yield g/plant)	
	Predicted	Observed	Predicted	Observed
1	25	34	35	33
2	30	40	36	37
3	41	48	35	34
4	36	45	33	31
5	30	37	40	42
6	32	39	42	45
7	36	42	42	40
8	23	32	27	30
9	29	41	29	32
10	31	38	32	31
11	37	45	34	33
12	33	42	33	31
13	33	37	37	38
14	39	43	29	31
15	25	34	36	39

the most sensitive indices for predicting LAI, chlorophyll content and biomass during *Kuruvai*, while PVI, MCARI and GNDVI exhibited higher correlation coefficients during *Navarai* season. Furthermore, stepwise multiple linear regression analysis revealed that a combined model incorporating LAI, SPAD chlorophyll and biomass yielded the highest coefficient of determination (R^2= 0.792 and 0.802) values for both reasons, indicating a robust predictive capability for rice yield. The predicted yield for the *Kuruvai* and *Navarai* seasons ranged from 25 to 39 and 29 to 42 g/plant, respectively. The generated yield was validated against observed yield data, confirming the reliability and accuracy of the predictive models.

The potential of drone-based vegetation indices as valuable tools for monitoring crop health, estimating biomass, and predicting rice yield with high precision. These advanced techniques offer a non-destructive, scalable and cost-effective approach for optimizing agricultural practices, enhancing crop productivity and ultimately contributing to food security and sustainable agriculture. Future research could further refine and validate these predictive models across diverse agro-climatic regions and crop varieties to enhance their applicability and scalability.

Acknowledgements

We thank the Department of Remote Sensing and GIS, Centre for Water and Geospatial Studies, Tamil Nadu Agricultural University, Coimbatore, for financial assistance in conducting this research.

Authors' contributions

RT carried out the experiment observation and drafted the manuscript. DM guided the research by formulating the concept and approved the final manuscript. SP guided the research by formulating the research concept and helped secure funds. KPR participated in the data analysis and performed the statistical analysis. RK conceived of the study and participated in its design and coordination. APS participated in the data analysis and revised manuscript. All authors reviewed the results and approved the final version of the manuscript.

Compliance with ethical standards

Conflict of interest: The authors declare no conflict of interest.

Ethical issues: None

References

1. Pazhanivelan S, Geethalakshmi V, Tamilmounika R, Sudarmanian NS, et al. Spatial rice yield estimation using multiple linear regression analysis, semi-physical approach and assimilating SAR satellite-derived products with DSSAT crop simulation model. Agronomy. 2022;12(9):2008. https://doi.org/10.3390/agronomy12092008
2. Tamilmounika R, Pazhanivelan S, Ragunath KP, Sivamurugan AP, et al. Paddy area estimation in Cauvery Delta Region Using Synthetic Aperture Radar. International Journal of Environment, Ecology and Conservation. 2022;S517-22. http://doi.org/10.53550/EEC.2022.v28i01s.069
3. De Castro AI, Shi Y, Maja JM, Peña JM. UAVs for vegetation monitoring: Overview and recent scientific contributions. Remote Sensing. 2021;13(11):2139. https://doi.org/10.3390/rs13112139
4. Kazemi F, Ghanbari Parmehr E. Evaluation of RGB vegetation indices derived from UAV images for rice crop growth monitoring. ISPRS Annals of the Photogrammetry, Remote Sensing and Spatial Information Sciences. 2023;10:385-90. https://doi.org/10.5194/isprs-annals-X-4-W1-2022-385-2023
5. Marang IJ, Filippi P, Weaver TB, Evans BJ, Whelan BM, et al. Machine learning optimized hyperspectral remote sensing retrieves cotton nitrogen status. Remote Sensing. 2021;13(8):1428. https://doi.org/10.3390/rs13081428
6. Boiarskii B, Hasegawa H. Comparison of NDVI and NDRE indices to detect differences in vegetation and chlorophyll content. Journal of mechanics of continua and mathematical sciences. 2019;4:20-9. https://doi.org/10.26782/jmcms.spl.4/2019.11.00003
7. Shanmugapriya P, Latha KR, Pazhanivelan S, Kumaraperumal R, et al. Cotton yield prediction using drone derived LAI and chlorophyll content. Journal of Agrometeorology. 2022;24(4):348-52. https://doi.org/10.54386/jam.v24i4.1770
8. Yue J, Feng H, Yang G, Li Z. A comparison of regression techniques for estimation of above-ground winter wheat biomass using near-surface spectroscopy. Remote Sensing. 2018;10(1):66. https://doi.org/10.3390/rs10010066
9. Delegido J, Verrelst J, Rivera JP, Ruiz-Verdú A, Moreno J. Brown and green LAI mapping through spectral indices. International Journal of Applied Earth Observation and Geoinformation. 2015;35:350-8. https://doi.org/10.1016/j.jag.2014.10.001
10. Rouse Jr JW, Haas RH, Deering DW, Schell JA, Harlan JC. Monitoring the vernal advancement and retrogradation (green wave effect) of natural vegetation. Earth Resources And Remote Sensing 1974.
11. Gitelson AA, Kaufman YJ, Merzlyak MN. Use of a green channel in remote sensing of global vegetation from EOS-MODIS. Remote sensing of Environment. 1996;58(3):289-98. https://doi.org/10.1016/S0034-4257(96)00072-7

12. Huete AR. A soil-adjusted vegetation index (SAVI). Remote sensing of Environment. 1988;25(3):295-309. https://doi.org/10.1016/0034-4257(88)90106-X

13. Baret F, Guyot G. Potentials and limits of vegetation indices for LAI and APAR assessment. Remote sensing of Environment. 1991;35(2-3):161-73. https://doi.org/10.1016/0034-4257(91)90009-U

14. Qi J, Chehbouni A, Huete AR, Kerr YH, Sorooshian S. A modified soil adjusted vegetation index. Remote sensing of Environment. 1994;48(2):119-26. https://doi.org/10.1016/0034-4257(94)90134-1

15. Din M, Zheng W, Rashid M, Wang S, Shi Z. Evaluating hyperspectral vegetation indices for leaf area index estimation of *Oryza sativa* L. at diverse phenological stages. Frontiers in plant science. 2017;8:237162. https://doi.org/10.3389/fpls.2017.00820

16. Wang W, Sun N, Bai B, Wu H, et al. Prediction of wheat SPAD using integrated multispectral and support vector machines. Frontiers in Plant Science. 2024;15:1405068. https://doi.org/10.3389/fpls.2024.1405068

17. Vidican R, Mălinaș A, Ranta O, Moldovan C, Marian O, et al. Using remote sensing vegetation indices for the discrimination and monitoring of agricultural crops: a critical review. Agronomy. 2023;13(12):3040. https://doi.org/10.3390/agronomy13123040

18. Shanmugapriya P, Latha KR, Pazhanivelan S, Kumaraperumal R, et al. Spatial prediction of leaf chlorophyll content in cotton crop using drone-derived spectral indices. Current Science. 2022:1473-80. https://doi.org/10.18520/cs/v123/i12/1473-1480

19. Palaniswamy KM, Gomez KA. Length-width method for estimating leaf area of rice 1. Agronomy Journal. 1974;66(3):430-3.

20. Zarco-Tejada PJ, Diaz-Varela R, Angileri V, Loudjani P. Tree height quantification using very high-resolution imagery acquired from an unmanned aerial vehicle (UAV) and automatic 3D photo-reconstruction methods. European Journal of Agronomy. 2014;55:89-99. http://dx.doi.org/10.1016/j.eja.2014.01.004

21. Cao J, Gu Z, Xu J, Duan Y, et al. Sensitivity analysis for leaf area index (LAI) estimation from CHRIS/PROBA data. Frontiers of Earth Science. 2014;8:405-13. http://dx.doi.org/10.1007/s11707-014-0432-0

22. Mudereri BT, Dube T, Adel-Rahman EM, Niassy S, et al. A comparative analysis of planetscope and sentinel sentinel-2 space-borne sensors in mapping striga weed using guided regularised random forest classification ensemble. The International Archives of the Photogrammetry, Remote Sensing and Spatial Information Sciences. 2019;42:701-8. http://dx.doi.org/10.5194/isprs-archives-XLII-2-W13-701-2019

23. Gitelson AA. Wide dynamic range vegetation index for remote quantification of biophysical characteristics of vegetation. Journal of Plant Physiology. 2004;161(2):165-73. https://doi.org/10.1078/0176-1617-01176

24. Towers PC, Strever A, Poblete-Echeverría C. Comparison of vegetation indices for leaf area index estimation in vertical shoot positioned vine canopies with and without grenbiule hail-protection netting. Remote Sensing. 2019;11(9):1073. https://doi.org/10.3390/rs11091073

25. Hunt Jr ER, Doraiswamy PC, McMurtrey JE, Daughtry CS, et al. A visible band index for remote sensing leaf chlorophyll content at the canopy scale. International Journal of Applied Earth Observation and Geoinformation. 2013;21:103-12.

26. Friedman JM, Hunt Jr ER, Mutters RG. Assessment of leaf color chart observations for estimating maize chlorophyll content by analysis of digital photographs. Agronomy Journal. 2016;108(2):822-9. https://doi.org/10.2134/agronj2015.0258

27. Taskos DG, Koundouras S, Stamatiadis S, Zioziou E, et al. Using active canopy sensors and chlorophyll meters to estimate grapevine nitrogen status and productivity. Precision Agriculture. 2015;16:77-98. https://doi.org/10.1007/s11119-014-9363-8

28. Shang J, Liu J, Ma B, Zhao T, Jiao X, et al. Mapping spatial variability of crop growth conditions using RapidEye data in Northern Ontario, Canada. Remote Sensing of Environment. 2015;168:113-25. https://doi.org/10.1016/j.rse.2015.06.024

29. Kanke Y, Tubana B, Dalen M, Harrell D. Evaluation of red and red-edge reflectance-based vegetation indices for rice biomass and grain yield prediction models in paddy fields. Precision agriculture. 2016;17:507-30. https://doi.org/10.1007/s11119-016-9433-1

30. Khan MS, Semwal M, Sharma A, Verma RK. An artificial neural network model for estimating Mentha crop biomass yield using Landsat 8 OLI. Precision Agriculture. 2020;21:18-33. https://doi.org/10.1007/s11119-019-09655-9

31. Ranjan R, Chandel AK, Khot LR, Bahlol HY, et al. Irrigated pinto bean crop stress and yield assessment using ground based low altitude remote sensing technology. Information Processing in Agriculture. 2019;6(4):502-14. https://doi.org/10.1016/j.inpa.2019.01.005

32. Zhou L, Chen N, Chen Z, Xing C. ROSCC: an efficient remote sensing observation-sharing method based on cloud computing for soil moisture mapping in precision agriculture. IEEE Journal of selected topics in applied earth observations and remote sensing. 2016;9(12):5588-98. https://doi.org/10.1109/JSTARS.2016.2574810

33. Zhang PP, Zhou XX, Wang ZX, Mao W, et al. Using HJ-CCD image and PLS algorithm to estimate the yield of field-grown winter wheat. Scientific Reports. 2020;10(1):5173. https://doi.org/10.1038/s41598-020-62125-5

34. Lee DH, Shin HS, Park JH. Developing a p-NDVI map for highland kimchi cabbage using spectral information from UAVs and a field spectral radiometer. Agronomy. 2020;10(11):1798. https://doi.org/10.3390/agronomy10111798

35. Ashapure A, Jung J, Chang A, Oh S, et al. A comparative study of RGB and multispectral sensor-based cotton canopy cover modelling using multi-temporal UAS data. Remote Sensing. 2019;11(23):2757. https://doi.org/10.3390/rs11232757

36. Henebry GM, Viña A, Gitelson AA. The wide dynamic range vegetation index and its potential utility for gap analysis. 2004, 12, 50-56.

37. Li M, Wu J, Song C, He Y, Niu B,et al. Temporal variability of precipitation and biomass of alpine grasslands on the northern Tibetan plateau. Remote Sensing. 2019;11(3):360. https://doi.org/10.3390/rs11030360

38. Vélez S, Martínez-Peña R, Castrillo D. Beyond vegetation: A review unveiling additional insights into agriculture and forestry through the application of vegetation indices. J-Multidisciplinary Scientific Journal. 2023;6(3):421-36. https://doi.org/10.3390/j6030028

39. Kaufman YJ, Tanre D. Atmospherically resistant vegetation index (ARVI) for EOS-MODIS. IEEE Transactions on Geoscience and Remote Sensing. 1992;30(2):261-70. https://doi.org/10.1109/36.134076

40. Alves KS, Guimarães M, Ascari JP, Queiroz MF, Alfenas RF, et al. RGB-based phenotyping of foliar disease severity under controlled conditions. Tropical Plant Pathology. 1:1-3.

41. Pazhanivelan S, Kumaraperumal R, Shanmugapriya P, Sudarmanian NS, et al. Quantification of Biophysical Parameters and Economic Yield in Cotton and Rice Using Drone Technology. Agriculture. 2023;13(9):1668. https://doi.org/10.3390/agriculture13091668

42. Utari D, Kamal M, Sidik F. Above-ground biomass estimation of mangrove forest using WorldView-2 imagery in Perancak Estuary, Bali. InIOP Conference Series: Earth and Environmental Science 2020;500(1):012011. https://doi.org/10.1088/1755-1315/500/1/012011

43. Adak A, Murray SC, Božinović S, Lindsey R, Nakasagga S, et al. Temporal vegetation indices and plant height from remotely sensed imagery can predict grain yield and flowering time breeding value in maize via machine learning regression. Remote Sensing. 2021;13(11):2141. https://doi.org/10.3390/rs13112141

44. Shamshiri RR, Mahadi MR, Ahmad D, Bejo SK, Aziz SA, et al. Controller design for an osprey drone to support precision agriculture research in oil palm plantations. In2017 ASABE Annual International Meeting 2017 (2-13).

45. Gitelson AA, Viña A, Verma SB, Rundquist DC, Arkebauer TJ, et al. Relationship between gross primary production and chlorophyll content in crops: Implications for the synoptic monitoring of vegetation productivity. Journal of Geophysical Research: Atmospheres. 2006;111(D8). https://doi.org/10.1029/2005JD006017

46. Baloloy AB, Blanco AC, Candido CG, Argamosa RJ, et al. Estimation of mangrove forest aboveground biomass using multispectral bands, vegetation indices and biophysical variables derived from optical satellite imageries: Rapideye, planetscope and sentinel-2. ISPRS annals of the photogrammetry, remote sensing and spatial information sciences. 2018;4:29-36. https://doi.org/10.5194/isprs-annals-IV-3-29-2018

47. Théau J, Gavelle E, Ménard P. Crop scouting using UAV imagery: a case study for potatoes. Journal of Unmanned Vehicle Systems. 2020;8(2):99-118. https://doi.org/10.1139/juvs-2019-0009

48. Pagola M, Ortiz R, Irigoyen I, Bustince H, Barrenechea E, et al. New method to assess barley nitrogen nutrition status based on image colour analysis: Comparison with SPAD-502. Computers and Electronics in Agriculture. 2009;65(2):213-8. https://doi.org/10.1016/j.compag.2008.10.003